Biochimica et Biophysica Acta 1837 (2014) 1699–1706

Contents lists available at ScienceDirect

Biochimica et Biophysica Acta

journal homepage: www.elsevier.com/locate/bbabio

Imaging mass spectrometry reveals fiber-specific distribution of acetylcarnitine and contraction-induced carnitine dynamics in rat skeletal muscles

Yasuro Furuichi [a], Naoko Goto-Inoue [a,b,*], Yasuko Manabe [a], Mitsutoshi Setou [b], Kazumi Masuda [c], Nobuharu L. Fujii [a,**]

[a] Department of Health Promotion Sciences, Graduate School of Human Health Sciences, Tokyo Metropolitan University, Tokyo, Japan
[b] Department of Cell Biology and Anatomy, Hamamatsu University School of Medicine, Hamamatsu, Japan
[c] Faculty of Human Sciences, Kanazawa University, Kanazawa, Japan

ARTICLE INFO

Article history:
Received 28 January 2014
Received in revised form 12 May 2014
Accepted 21 May 2014
Available online 29 May 2014

Keywords:
Carnitine
Muscle contraction
Fiber type

ABSTRACT

Carnitine is well recognized as a key regulator of long-chain fatty acyl group translocation into the mitochondria. In addition, carnitine, as acetylcarnitine, acts as an acceptor of excess acetyl-CoA, a potent inhibitor of pyruvate dehydrogenase. Here, we provide a new methodology for accurate quantification of acetylcarnitine content and determination of its localization in skeletal muscles. We used matrix-assisted laser desorption/ionization imaging mass spectrometry (MALDI–IMS) to visualize acetylcarnitine distribution in rat skeletal muscles. MALDI–IMS and immunohistochemistry of serial cross-sections showed that acetylcarnitine was enriched in the slow-type muscle fibers. The concentration of ATP was lower in muscle regions with abundant acetylcarnitine, suggesting a relationship between acetylcarnitine and metabolic activity. Using our novel method, we detected an increase in acetylcarnitine content after muscle contraction. Importantly, this increase was not detected using traditional biochemical assays of homogenized muscles. We also demonstrated that acetylation of carnitine during muscle contraction was concomitant with glycogen depletion. Our methodology would be useful for the quantification of acetylcarnitine and its contraction-induced kinetics in skeletal muscles.

1. Introduction

Carnitine is a key factor in muscle cell metabolism, because it serves as a carrier for energy substrates through mitochondrial membranes. Carnitine is responsible for the translocation of long-chain acyl-CoAs derived from circulating lipids into the mitochondrial matrix where they enter the beta-oxidation pathway [1]. Long-chain acyl-CoAs are converted to acylcarnitines by carnitine palmitoyltransferase 1, which is located at the outer mitochondrial membrane [2]. Acylcarnitine can be transported via carnitine translocase, which re-converts acylcarnitine back to carnitine and long-chain acyl-CoAs, which can then be oxidized. Another major role of carnitine in skeletal muscles is to buffer excess carbon fuels. In cases where beta-oxidation outpaces metabolic flux through the tricarboxylic acid (TCA) cycle, short-chain acyl-CoA intermediates are accumulated in muscle mitochondria [3]. This situation is reversed by carnitine acetyl-transferase (CrAT), which resides principally within the mitochondrial matrix where it acts selectively on short chain acyl-CoAs. CrAT converts the accumulating short chain (mainly C2–C10) acyl-CoA to acylcarnitine, which then exit the organelle and the tissue [4].

Acylcarnitine has been identified as a metabolic indicator, and serum and muscle acylcarnitine levels are known to reflect the metabolic state [5]. More specifically, the shortest acylcarnitine (acetylcarnitine, C2) is thought to be important for controlling metabolic flexibility because acetyl-CoA acts as a potent allosteric inhibitor of pyruvate dehydrogenase, a rate-limiting enzyme for pyruvate entry into the TCA cycle [6]. Additionally, over-accumulation of acetyl-CoA in muscle-specific CrAT-deficient mice was observed in the mitochondria and the mice showed glucose intolerance and insulin resistance [4]. These findings suggest that acetylation of carnitine is a key factor of muscle metabolic flexibility.

Abbreviations: MALDI–IMS, matrix-assisted laser desorption/ionization imaging mass spectrometry; TCA, tricarboxylic acid; CrAT, carnitine acetyl-transferase; OCTN2, carnitine/organic cation transporter; *m/z*, mass-to-charge ratios; DHB, 2,5-dihydroxybenzoic acid; 9-AA, 9-aminoacridine; MALDI TOF/TOF, MALDI-time-of-flight/time-of-flight; MAS, Matsunami Adhesive Slide; H&E, hematoxylin and eosin; PAS, periodic acid-Schiff; MHC, myosin heavy chain

* Correspondence to: N. Goto-Inoue, Department of Health Promotion Science, Tokyo Metropolitan University, Minami-Osawa, Hachioji City, Tokyo 192-0397, Japan. Tel.: +81 42 677 2965; fax: +81 42 677 2961.
** Corresponding author at: N.L. Fujii, Department of Health Promotion Science, Tokyo Metropolitan University, Minami-Osawa, Hachioji City, Tokyo 192-0397, Japan. Tel.: +81 42 677 2966; fax: +81 42 677 2961.
E-mail addresses: naokog@tmu.ac.jp (N. Goto-Inoue), fujiin@tmu.ac.jp (N.L. Fujii).

http://dx.doi.org/10.1016/j.bbabio.2014.05.356
0005-2728/

The ratio of acetylcarnitine to carnitine in skeletal muscles is increased in situations of enhanced fatty acid oxidation induced by lipid infusion [7,8]. Additionally, high-intensity exercise increases acetylcarnitine accumulation resulting from increased pyruvate dehydrogenase activity following enhanced glycolysis [9]. In these situations, total carnitine content (sum of free-, acetyl-, and acyl-carnitine) does not change [9], indicating that carnitine is converted to acetylcarnitine in muscle cells. Changes in carnitine and acetylcarnitine contents have been generally evaluated by enzymatic assay on the basis of the measurement of CrAT activity [10,11]. A critical limitation of this assay is that acetylcarnitine cannot be distinguished from other acylcarnitines because CrAT has affinity for varying the length of acyl-CoA ranging from C2 (acetyl-CoA) to C10 [12]. For precise evaluation of acetylcarnitine levels, liquid chromatography electrospray ionization mass spectrometry has been used [11]. Previous studies have comprehensively evaluated tissue carnitine species and distinguished acetylcarnitine from the other acylcarnitines using this method [13]. However, using this method entails extraction and purification steps, which lead to loss of information on carnitine-distribution in biological tissue.

In skeletal muscles, carnitine metabolism is presumed to be associated with muscle characteristics. Skeletal muscle is composed of heterogeneous fiber types, which are mainly distinguished into type I fibers (slow and oxidative) or type II fibers (fast and glycolytic). We have previously demonstrated that carnitine uptake capacity and its transporter OCTN2 (carnitine/organic cation transporter) expression were higher in oxidative muscles than in glycolytic muscles, suggesting that carnitine metabolism is higher in type I fibers in which mitochondria are abundant [14]. However, it remains unknown whether carnitine content and carnitine acetylation depend on fiber type-specific characteristics because no method shows the localization of carnitine molecule in tissues precisely.

Here, we used matrix-assisted laser desorption/ionization imaging mass spectrometry (MALDI–IMS), which integrates microscopy and mass spectrometry, for label-free, ex vivo visualization of acetylcarnitine localization. This technique enables the discrimination of acetylcarnitine from other species of acylcarnitine by determining the differences in mass-to-charge ratios (m/z). The purpose of this study was to determine the localization of acetylcarnitine in rat skeletal muscles and evaluate changes in carnitine dynamics induced by muscle contraction using MALDI–IMS. Our results showed that distribution of acetylcarnitine was primarily in the slow-type fibers, where high metabolic activity was detected based on ATP concentration. We also demonstrated that muscle contraction increased acetylcarnitine in a specific part of muscles, which is concomitant with glycogen depletion.

2. Materials and methods

2.1. Materials

The matrices, 2,5-dihydroxybenzoic acid (DHB), and 9-aminoacridine (9-AA), were purchased from Bruker Daltonics (Bremen, Germany) and Merck Schuchardt (Hohenbrunn, Germany), respectively. Methanol, ethanol, and ultra-pure water (Wako Pure Chemical Industries, Osaka, Japan) were used for the preparation of all buffers and solvents. All chemicals used in this study were of the highest purity available. The monoclonal antibodies used in this study were purchased from Sigma (St. Louis, MO) and DSHB (Iowa City, IA).

2.2. Animals and in situ contraction

Care and use of laboratory animals were in accordance with the Experimental Animal Committee of Tokyo Metropolitan University and we followed the Guidelines for the Proper Conduct of Animal Experiments established by the Science Council of Japan.

In situ contractions were performed as previously described [15] with some modifications. Briefly, male Wistar rats weighing 250–300 g were anesthetized with sodium pentobarbital (50 mg kg^{-1} intraperitoneally). Approximately 3 h prior to the experiment, the chow was removed from the cages in order to eliminate the influence of feeding. After the lower legs were shaved and cleaned, a surfaced electrode (Vitrode, Nihon Kohden, Tokyo, Japan) was attached to the proximal and distal regions of the calf muscle. Under resting conditions, the right and left ankles and knee joints were fixed at 90°. Isometric, tetanic muscle contractions were elicited in the left leg by electrostimulation via a surface electrode with trains of stimuli (0.2-ms pulse duration at 40 Hz, 10 V, lasting for 0.2 s). The calf muscles (lateral and medial gastrocnemius and soleus) were stimulated. The stimulation was applied at a rate of one contraction per second for 5 min or 30 min. The contralateral leg was considered as the resting leg. Following contraction, muscle tissues were immediately dissected and frozen in 2-methylbuthane and stored at −80 °C without fixation.

2.3. Measurement of muscle carnitine and glycogen content

For measurement of carnitine content, rat gastrocnemius muscle was separated into its surface and deep portions. The deep portion of gastrocnemius muscle, which is enriched with myoglobin, was identified visually by its red tissue color; the surface portion was white in color. Surface and deep portions are characterized as glycolytic and oxidative muscles, respectively [16]. The isolated muscles were minced on ice, homogenized in 3% perchloric acid and centrifuged at 1000 ×g for 10 min. The supernatant was neutralized with 2.5 M K_2CO_3 and centrifuged at 1000 ×g. Total and free carnitine contents were determined by the enzymatic cycling method (total and free carnitine assay kits, Kainos). The acylcarnitine content was calculated from the difference between total acid soluble and free carnitine [17].

For glycogen measurements, 10 mg of muscle tissue was hydrolyzed in 2 M HCl and neutralized by adding 2 M NaOH, and then the supernatant was used for glucose analysis. Glucose levels were determined using a hexokinase-dependent assay kit according to the manufacturer's instructions (GAHK-20, Sigma).

2.4. Histochemical analysis

Sections were prepared as described previously [18]. Briefly, consecutive 10-μm sections were cut using a cryostat (CM 1850; Leica Microsystems, Wetzlar, Germany). The serial sections were mounted onto Matsunami Adhesive Slide-(MAS) coated slides (Matsunami, Osaka, Japan) for histochemical staining, and indium-tin oxide-coated glass slides (Bruker Daltonics) for imaging mass spectrometry. For morphological observation, sections were stained with hematoxylin and eosin (H&E). To evaluate glycogen content, the serial sections were stained with periodic acid-Schiff stain (PAS, Millipore).

2.5. Immunohistochemical analysis

For the determination of muscle-fiber type, sections were stained with antibodies against myosin heavy chains. Tissue sections were fixed in 4% paraformaldehyde/phosphate buffer and incubated with primary antibodies against myosin heavy chain (MHC) type I (M8421, Sigma), MHC II (M4276, Sigma), and MHC I + IIa (BF-32, DSHB) and then visualized using appropriate species-specific Alexa Fluor 488 fluorescence-conjugated secondary antibodies (Invitrogen). The fluorescence was detected with a wide field fluorescence microscope (Keyence, Osaka, Japan). To classify the fiber types, the images of MHC expression visualized using immunohistochemistry were converted to black-and-white using ImageJ software (NIH, Bethesda, MD).

2.6. Imaging mass spectrometry

Before imaging analysis was performed, tissue sections were covered with matrices. We detected carnitine species in positive-ion mode where the molecules are detected as either the radical cations or the protonated molecules. On the other hand, we measured nucleotides in a negative-ion mode – where sample molecules are converted to radical anions through absorption of electrons [19] – because a previous report showed that these metabolites were sensitively detected in this mode [20]. For MALDI–MS in positive-ion mode, 50 mg/mL of DHB in methanol/water (7/3, v/v) was sprayed uniformly over the sections with a 0.2-mm nozzle caliber airbrush (Procon Boy FWA Platinum; Mr. Hobby, Tokyo, Japan). For MALDI–MS in negative-ion mode, 9-AA was prepared at a concentration of 10 mg/mL in ethanol/water (7/3, v/v) and used as a matrix. Imaging analysis was performed using a MALDI-time-of-flight/time-of-flight (MALDI–TOF/TOF) instrument, the Ultraflex II (Bruker Daltonics), as described previously [18] with minor modifications. The instrument was equipped with a 355-nm neodymium-doped yttrium aluminum garnet (Nd/YAG) laser with a repetition rate of 200 Hz. The laser irradiated the tissue sections 200 times per position. All pixels were 200 μm. The mass spectrometry parameters were set to obtain the highest sensitivity with m/z values in the range of 40–600 in positive-ion mode and 200–1000 in negative-ion mode. FlexImaging software (Bruker Daltonics) was used for automatic acquisition of the spectra, reconstruction of the ion images, and for total ion current normalization.

2.7. Tandem mass spectrometry

For the tandem mass spectrometric analysis (MS/MS), a QSTAR Elite high-performance, hybrid quadrupole TOF mass spectrometer (Applied Biosystems, Foster City, CA) was used according to a previously described procedure [21]. The MS/MS analysis was performed directly on tissue sections of the skeletal muscle. Collisional activation of selected ions was carried out using relative collision energy with argon as the collision gas. The conditions for data acquisition (laser power and collision energy) were changed in order to obtain product-ion mass spectra with peaks that had high intensity and a high signal-to-noise ratio [21].

2.8. Data analysis

Energy charge was assigned as ([ATP] + 0.5 [ADP])/([ATP] + [ADP] + [AMP]) [22], and calculated using SIMenergy software (Shimadzu co., Kyoto, Japan) that is currently under development. All data are expressed as mean ± standard error of the mean (SEM). Paired t-test was used to compare the basal and contracted muscles. Variables among fiber types were compared using one-way analysis of variance (ANOVA). Tukey–Kramer post hoc test was conducted if the ANOVA indicated a significant difference. The level of significance was set at $p < 0.05$.

3. Results

3.1. Muscle carnitine content

We measured free carnitine and acyl + acetyl carnitine contents based on enzymatic cycling in the surface and deep portions of gastrocnemius muscle in the resting rat legs. Although there was no significant difference in free carnitine content between the surface and deep portions, acylcarnitine content was higher in the deep portion when compared to the surface portion of gastrocnemius muscle (Fig. 1), which is in accordance with previous reports [14]. However, this method was not able to determine which acylcarnitines were accumulated in the deep portion of gastrocnemius muscle. Therefore, we next tried to measure the precise acetylcarnitine content, without the contamination of other short chain acylcarnitines, using mass spectrometry.

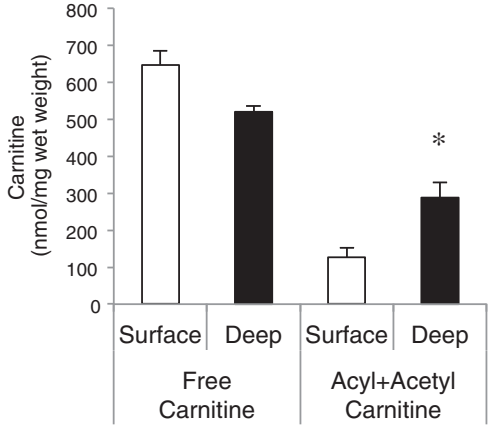

Fig. 1. Comparison of muscle carnitine and the sum of acyl and acetylcarnitine content in the surface and deep portions of rat gastrocnemius muscle, measured by enzymatic analysis. Values are presented as mean ± SEM from 3 animals. *: $p < 0.05$ vs. surface portion of muscle.

3.2. MALDI–IMS carnitine imaging

To quantify carnitine and visualize its distribution directly, we performed MALDI–IMS analyses using sections of gastrocnemius muscles. Fig. 2a represents the distributions of protonated $[M + H]^+$ ions derived from carnitine at m/z 162.2 and acetylcarnitine at m/z 204.2. It was observed that carnitine was distributed throughout the entire gastrocnemius muscle, while acetylcarnitine was localized in a specific region of gastrocnemius muscle. To identify these molecules, we used a MS/MS. The fragmentation spectra of these carnitine species were detected by MALDI–MS/MS directly from the gastrocnemius muscle sections (Fig. 2b). We confirmed that carnitine is fragmented to a main product ion at m/z 103, resulting from the loss of the trimethyl amine group. Similar to previous reports [23], we also monitored the two main product ions at m/z 145 and 85 from acetylcarnitine by performing MS/MS.

Since acetylcarnitine was detected in a specific region of gastrocnemius muscle, we investigated the correlative distribution between muscle fiber type and acetylcarnitine in serial sections through immunohistochemical analysis. Four subpopulations of fiber type, referred to as type I, II, I + IIa, and others (mainly IIb), were identified. Sections were stained with the antibody specific to slow-type MHC, fast-type MHC, and the BF32 antibody, which reacts with type I and IIa MHC (does not react with IIb and IIx) [24]. Identification of muscle fibers revealed that acetylcarnitine is enriched in type I fibers (Fig. 3a). To semi-quantify the apparent fiber-specific distribution of acetylcarnitine, a region of each fiber type was selected according to the images of immunohistochemical analysis. Averaged spectra from each region were generated, and compared among fiber types as previously shown [25–27]. Fig. 3b shows the semi-quantitative comparison of carnitine and acetylcarnitine between different regions representative of different fiber types. Averaged spectra from the type I fiber-enriched region was considered 100%, and the values for other fibers were expressed as a proportion of this. Although there were no differences in carnitine contents between regions, acetylcarnitine was significantly greater in type I fiber-enriched areas than in regions of type II and IIb fibers (Fig. 3a, b).

We detected two other acylcarnitine species: octanoylcarnitine at m/z 288.4 and palmitoylcarnitine at m/z 400.6. Although the octanoylcarnitine concentration was quite low, the palmitoylcarnitine concentration was 10–50% of the acetylcarnitine concentration and was distributed in regions enriched with type I fibers (Supplementary Fig. 1).

3.3. Energy charge in different fiber types

To evaluate the energy charge in different types of skeletal muscle fibers, we examined ions related to adenosine phosphates AMP, ADP,

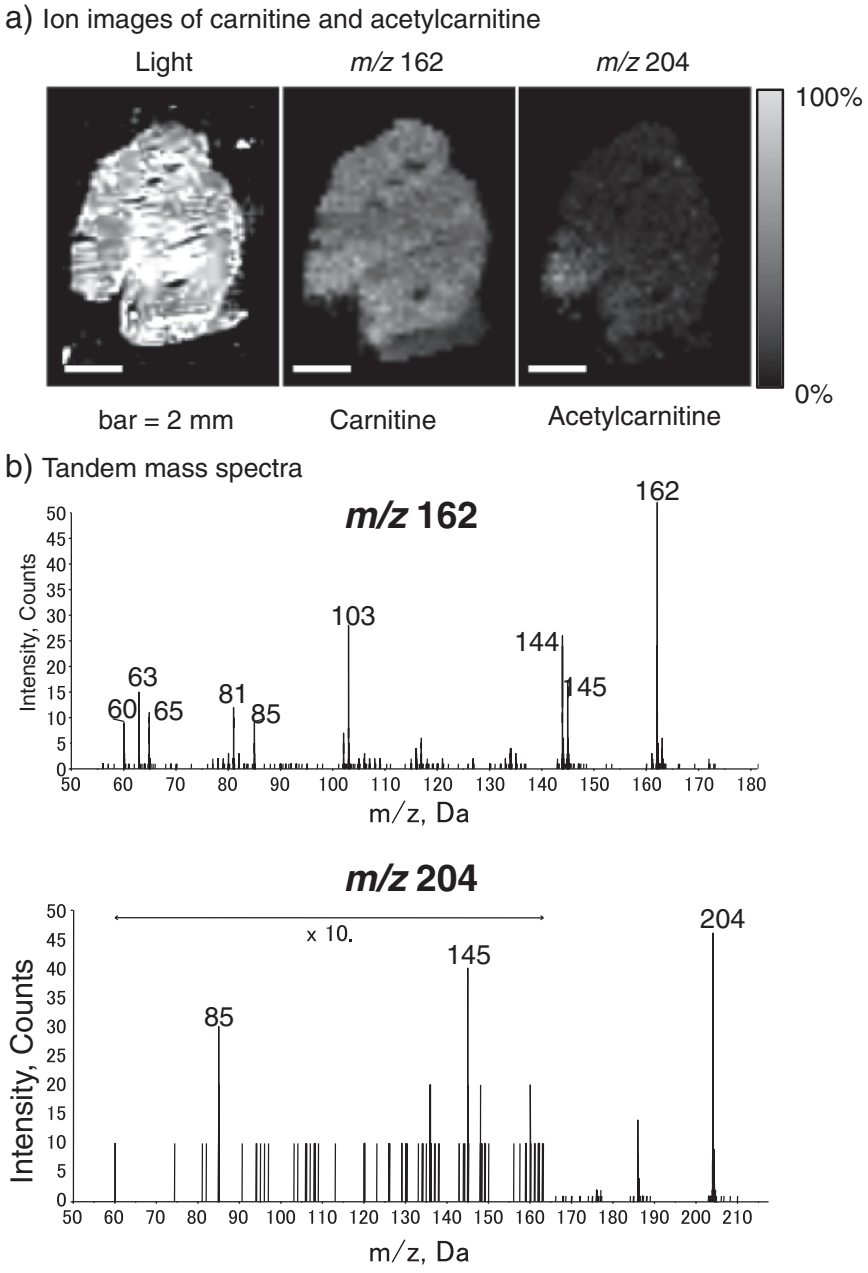

Fig. 2. Visualization of carnitine and acetylcarnitine in rat gastrocnemius muscle sections using imaging mass spectrometry analysis. (a) Optical image of muscle before IMS and ion images of each *m/z* value in positive-ion mode. Optical images acquired under bright-field. Mass spectrometric images of carnitine at *m/z* 162 and acetylcarnitine at *m/z* 204. (b) Tandem mass spectrometric analysis was performed and the fragmentation spectra of carnitine and acetylcarnitine were detected in tissue sections of each condition.

and ATP [18]. As shown in Fig. 4, ATP, ADP, and AMP-related ions were detected in negative-ion mode, and the energy charge was calculated in each pixel by a formula proposed by Atkinson [22]. Low energy charge signal indicates decreased ATP to ADP ratio, representing up-regulation of metabolic activities. We found that energy charge was lower in specific areas, suggesting the regiospecificity of metabolic activity in rat gastrocnemius muscle. We then identified the fiber type of this muscle section using immunohistochemistry and revealed that the energy charge was lower in type I fibers (Fig. 4). The histogram shows that the energy charge was low in type I fibers, and high in type II fibers, suggesting that metabolic activity was up-regulated in type I fibers. These data indicated that acetylcarnitine is enriched in the slow-type regions with up-regulated metabolic state.

3.4. Effects of in situ muscle contraction on metabolism

Exercise has been shown to increase acetylcarnitine content in skeletal muscles for buffering excess carbon fuel [28]. Therefore, we examined the effect of muscle contraction on carnitine metabolism in skeletal muscles. To confirm the adequacy of our in situ contraction model, we measured the muscle glycogen content by histochemical and biochemical analyses. Fig. 5a shows the H&E stained images of muscle to identify the morphological differences between basal and contracted tissues (contraction). There were no obvious differences in myofiber conditions between the tissues. On the other hand, PAS staining, which detects glycogen in tissues, revealed that muscle glycogen levels decreased after 30 min of muscle contraction (Fig. 5a). We also measured glycogen content in homogenated muscles from contracted

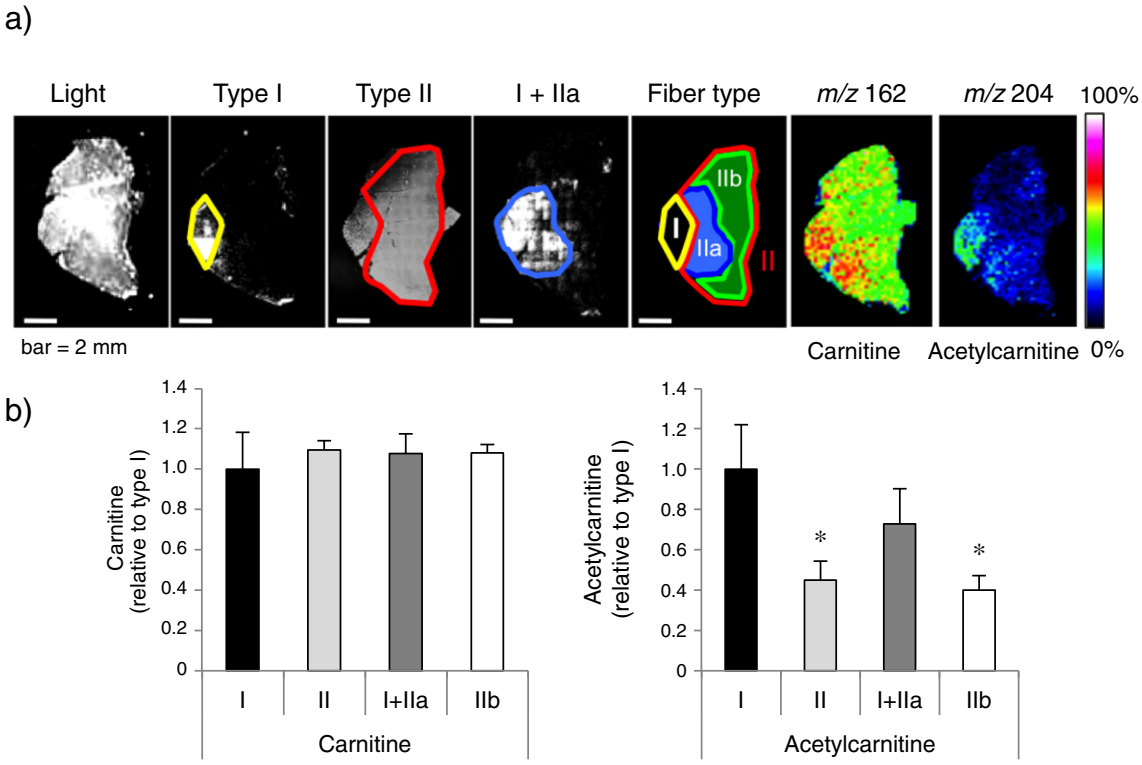

Fig. 3. Identification of muscle fiber type in serial section of muscles (a) and quantification of carnitine and acetylcarnitine in each fiber type (b). (a) Serial sections were stained with antibodies against MHC I, II, or I + IIa. Four sub-populations of fiber type in the muscle section were determined by immunohistochemical images. It is assumed that type I (yellow), type II (red), type I + IIa (blue), and type IIb (green) were abundant in each colored area. (b) Carnitine and acetylcarnitine intensity were quantified in each fiber type. Quantification of the molecules are expressed relative to the type I fibers. Values are presented as mean ± SEM from 3 animals. *: $p < 0.05$ vs. type I.

and basal tissues with a biochemical method, and confirmed that glycogen content was decreased in contracted muscle (Fig. 5b). However, changes in carnitine and acylcarnitine levels following muscle contraction could not be detected in the enzymatic assay (Fig. 5c).

3.5. MALDI–IMS carnitine imaging after muscle contraction

It is essential to differentiate the kinetics of acetylcarnitine from other species of acylcarnitine to understand the roles of carnitine in the regulation of muscle metabolism. Therefore, we performed MALDI–IMS and evaluated the changes in carnitine and acetylcarnitine in the skeletal muscle caused by electrical pulse-evoked contraction. Fig. 6 shows the MALDI–IMS results of carnitine and acetylcarnitine in rested right leg (basal) and contracted left leg (contraction) after 5-min and 30-min muscle contractions. It was shown that acetylcarnitine is enriched in the type I fibers in both basal and contracted muscles after 5-min electrical stimulation (Fig. 6a), indicating that acetylcarnitine levels did not change following a short-term contraction. On the other hand, we

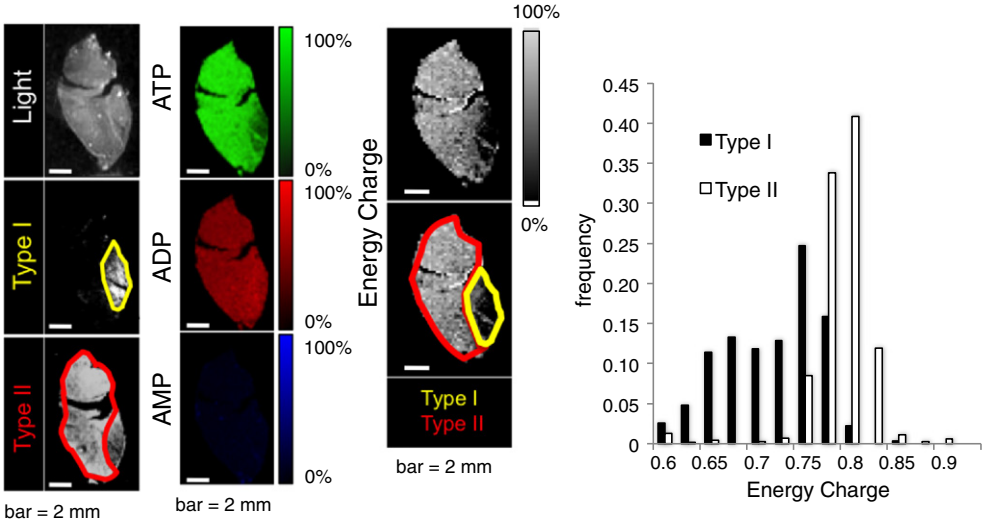

Fig. 4. Identification of fiber type by immunohistochemistry and ion images of each *m/z* value in negative-ion mode. In negative-ion mode, ATP, ADP, and AMP distribution were visualized in the rat gastrocnemius tissue. Red and yellow circles indicate the type I and II fiber respectively. Energy charge was calculated and visualized using the SIMenergy software (Shimadzu Co., Japan). The histogram was calculated examining each pixel.

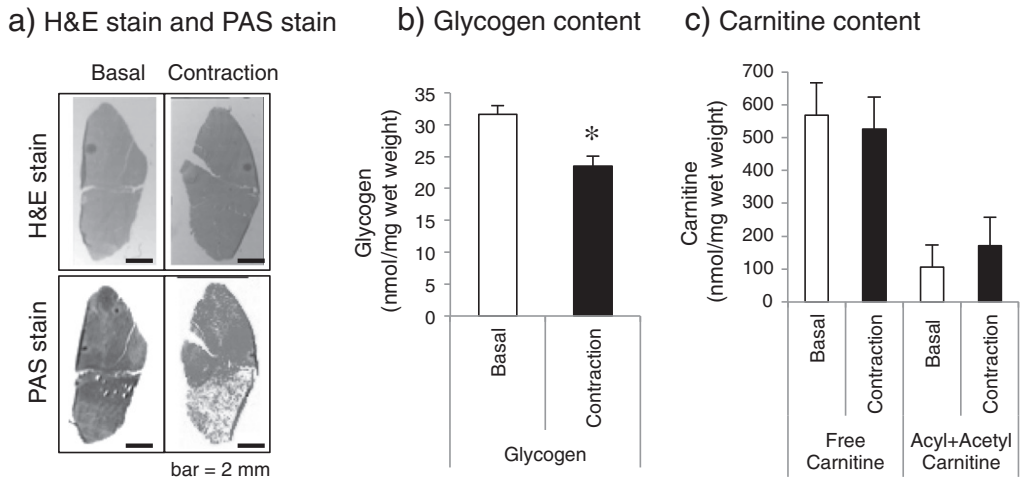

Fig. 5. Effect of muscle contraction on glycogen and carnitine contents in rat gastrocnemius muscles. (a) H&E- and PAS-stained images in basal and contracted muscles are shown. (b) Glycogen content in basal and contracted muscles measured by the biochemical method. Values are presented as mean ± SEM from 6 animals. *: $p < 0.05$ vs. basal muscles. (c) Comparison of free carnitine and acylcarnitine contents in basal and contracted muscles. Values are presented as mean ± SEM from 6 animals. There were no significant differences from muscle contraction.

found that acetylcarnitine signal increased in contracted muscle after 30 min, while there was no change in contralateral basal muscles (Fig. 6b). Indeed, the average spectra of acetylcarnitine in whole sections of contracted muscles were significantly greater (3.2-fold) than those of basal muscles (Fig. 6b). Unlike acetylcarnitine, there was no change in palmitoylcarnitine content after muscle contraction (Supplementary Fig. 2). To examine the correlative distribution of acetylcarnitine accumulation and muscle fiber type, we analyzed the serial sections through immunohistochemistry. Contrary to expectation, acetylcarnitine increases were not fiber type-dependent. To confirm whether the acetylcarnitine accumulation was involved in muscle contractile activity, we compared MALDI–IMS images with PAS staining. We found that acetylcarnitine-enriched regions overlapped with glycogen-depleted regions, as indicated by black arrows (Fig. 6b).

4. Discussion

In the current study, we successfully evaluated acetylcarnitine content and its distribution in rat gastrocnemius muscle using MALDI–IMS. Since this imaging technique enabled retention of information of

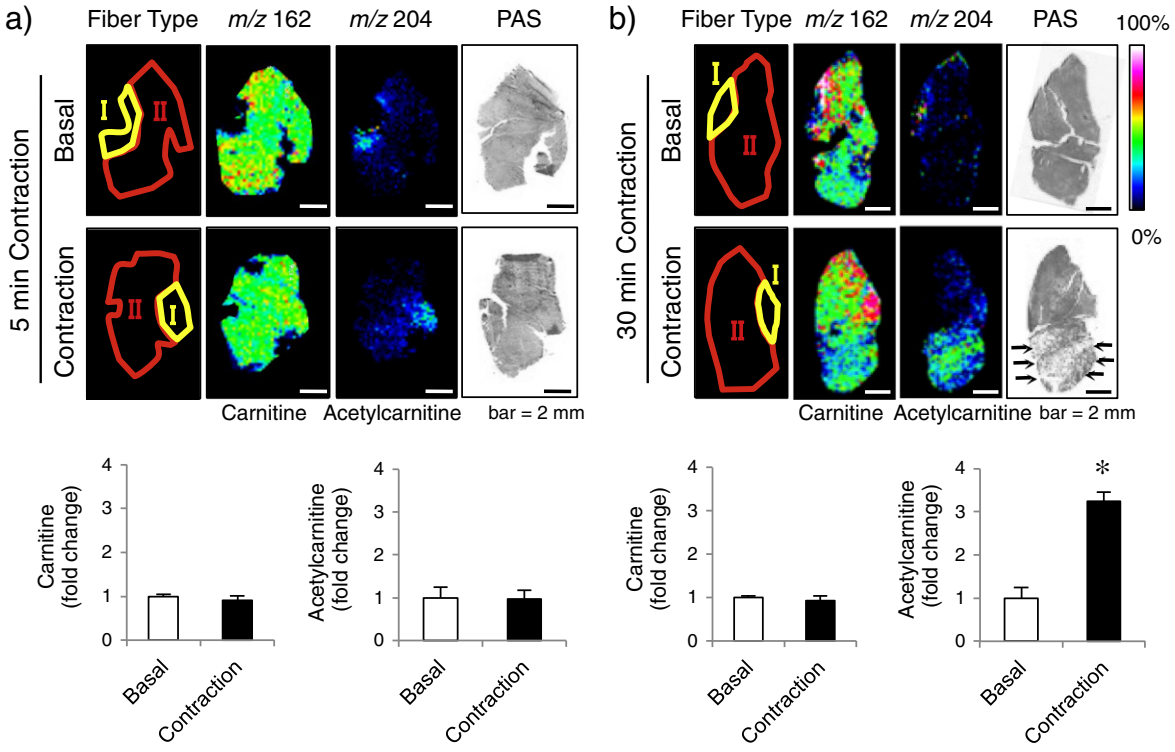

Fig. 6. Effect of muscle contraction on carnitine and acetylcarnitine distribution evaluated by MALDI–IMS in basal and contracted muscles. Each fiber type is shown in the left panels as type I (yellow) and type II (red). (a) Five minutes of electrical stimulation did not change the carnitine and acetylcarnitine distribution. Quantification of data is shown at the bottom. Values are expressed relative to the basal muscles and presented as mean ± SEM from 3 animals. (b)30 min of electrical stimulation induced the change in acetylcarnitine distribution. Acetylcarnitine is increased in contracted muscles. Increase in acetylcarnitine levels is accompanied with glycogen depletion, as shown in PAS staining. Values are presented as mean ± SEM from 6 animals. *: $p < 0.05$ vs. basal muscle.

molecule localization in biological tissues, it was clearly shown that acetylcarnitine is abundant in type I fibers in basal states. Moreover, we showed that in situ muscle contraction increased acetylcarnitine content, which was concomitant with depletion of muscle glycogen, suggesting the tight coupling of acetylcarnitine accumulation and the contractile activity of muscle fibers. At the initial phase of muscle contraction (5-min contraction), acetylcarnitine content did not change, but increased drastically after an additional 25 min of contraction in rat skeletal muscle. Acetylcarnitine accumulation during muscle contraction is presumed to be the excess production of acetyl-CoA during glycolysis, which exceeds the tissue's demand. We observed that the location of acetylcarnitine accumulation matched with the region of increased energy utilization due to muscle contraction, suggesting that carnitine functions as an acceptor of excess acetyl-CoA and contributes to metabolic flexibility.

In previous reports, tissue acetylcarnitine level has primarily been estimated by radioisotopic assays in which the amount of radiolabeled metabolites reacting with CrAT in homogenized samples [10,11]. It was recently demonstrated, however, that CrAT has specificity not only to acetylcarnitine (C2) but also to propionylcarnitine (C3) or butyrylcarnitine (C4) [12]. MALDI–IMS, the method we used in this report, directly measures the acetylcarnitine molecule, showing the precise acetylcarnitine amount without contamination by other short-chain acylcarnitines. Indeed, we detected other acylcarnitines (octanoylcarnitine and palmitoylcarnitine) and found that the palmitoylcarnitine concentration was approximately 40% of the acetylcarnitine level in type I fibers. Therefore, it is likely that enzymatic assays overestimate the concentration of acetylcarnitine. To confirm the accuracy of the detected molecular peaks of the acetylcarnitine ion, we performed tandem mass spectrometry and detected the fragmented ions (Fig. 2b). The results matched the theoretical fragmented ions derived from acetylcarnitine, indicating the detected signal is indeed the target molecule [23,29]. Additionally, since extraction and purification processes are not necessary for MALDI–IMS, quantification of the metabolite is more efficient when compared to classical methods. While there are various methods to quantify carnitine species in biological tissues [11], MALDI–IMS is a simple and powerful tool for evaluating acetylcarnitine distribution.

Interestingly, it was revealed that acetylcarnitine was localized in a specific region of rat gastrocnemius muscles in basal states; therefore, we tried to separate the muscle fiber types and compare relative amounts of acetylcarnitine between fiber types. Skeletal muscle fibers are generally categorized into three types, slow oxidative (type I), fast oxidative glycolytic (type IIa), and fast glycolytic (type IIb) [16]. We separated deep and surface portions of rat gastrocnemius muscles by visual assessment and showed high acetylcarnitine concentration in the deep portion. The deep portion of gastrocnemius muscle consists of oxidative muscle fibers (type I and type IIa). We also determined a type I fiber-enriched area by immunohistochemical analysis and quantified the acetylcarnitine content of the serial sections. Our data clearly showed that acetylcarnitine is abundantly distributed in type I fibers and at relatively lower levels in type IIa fibers. This is the first report of visualization of acetylcarnitine distribution and quantification of its content in different muscle fiber types using histological techniques.

To determine the relationship between acetylcarnitine distribution and muscle metabolic activity, we evaluated the energy charge, an index of metabolic activity [22]. It was demonstrated that the energy charge was lower in type I fibers compared to type II fibers, representing that metabolic activity is higher in slow type fibers. Since type I fibers have more mitochondria and a higher capacity for beta-oxidation [16], they accumulate acetyl-CoA under resting conditions. Excess acetyl-CoA is converted to acetylcarnitine, because acetyl-CoA acts as an allosteric inhibitor of pyruvate dehydrogenase. Therefore, our finding that acetylcarnitine distribution corresponds to metabolic activity indicates the physiological significance of carnitine buffering excess acetyl-CoA in order to maintain appropriate levels of acetyl-CoA in mitochondria. Our data suggest that type I fibers are highly adaptable to utilizing lipids and carbohydrates as fuels and transitioning between the two, a feature known as metabolic flexibility [30].

In order to clarify the effect of muscle contraction on intramuscular carnitine metabolism, we performed electrostimulation on rat gastrocnemius muscles and compared the carnitine contents between basal and contracting muscles. Although there were no changes in acetylcarnitine content in muscles after 5-min contraction, acetylcarnitine levels in the whole section increased about 3.2-fold in contracting muscles after 30 min of contraction. In contrast to acetylcarnitine, there was no change in palmitoylcarnitine content after muscle contraction, suggesting that contraction-induced acetylcarnitine accumulation was not the result of beta-oxidation but rather glucose oxidation. Moreover, we found that acetylation of carnitine occurred locally, and were not fiber type-dependent. Inconsistent with our data, a previous report indicated that the accumulation of acetylcarnitine during voluntary cycling exercise was higher in type I fibers than in type II fibers, based on biopsy of human vastus lateralis muscles [31]. This discrepancy likely resulted from the difference in the types of muscle contractions studied (i.e., voluntary exercise vs. forced contraction by electrical stimulation). In the present study, the surface area of the gastrocnemius was preferentially activated, as shown by the PAS stain (Fig. 6b). This indicates relatively low activation of the muscle area containing the highest proportion of type I fibers.

In the present study, we demonstrated that contraction-induced carnitine acetylation overlapped with glycogen depletion, suggesting that carnitine acetylation depends on increased metabolic activity [32]. Importantly, we measured the change in acetylcarnitine concentration of homogenized muscle samples by enzymatic methods, but did not detect a significant change. This discrepancy is likely explained by contamination by other acylcarnitine species in the enzymatic analysis. Furthermore, contraction-induced carnitine kinetics is limited to the specific region and is undetectable when analyzing whole homogenized muscles. Imaging techniques are beneficial, not only for accuracy, but also for detecting the local dynamics of metabolite distribution, which could not be observed with general biochemical assays.

It is important to note the biological meaning of acetylcarnitine production during muscle contraction. As mentioned above, carnitine functions as an acceptor for excess acetyl-CoA and relieves the inhibition of glucose oxidation. In addition, it has been hypothesized that acylcarnitine is exported from muscle cells following the increase of intracellular acylcarnitine concentration and acts as a biologically active substrate [13]. Recently, it has been reported that acetylcarnitine is a potentially beneficial molecule in the treatment of various neurological diseases such as Alzheimer's disease [33], implying the inter-organ shuttle of carnitine systems. Interestingly, it has been reported that plasma acetylcarnitine concentration increased during human exercise [28], suggesting the possibility that accumulated acetylcarnitine might be exported during muscle contraction. Further study is needed to elucidate the export of acetylcarnitine during muscle contraction and to determine its physiological significance.

In conclusion, we showed the fiber-specific acetylcarnitine distribution of rat skeletal muscles using MALDI–IMS techniques. By identification of fiber type using immunohistochemical analysis in serial sections, we revealed that acetylcarnitine is enriched in type I fibers under basal state. Acetylcarnitine is accumulated during contraction in skeletal muscle, and this region of acetylcarnitine accumulation corresponds to regions of glycogen depletion, suggesting carnitine acetylation occurs with a high degree of metabolic demand induced by sustained muscle contraction. Further investigations are required to elucidate the physiological meaning of contraction-induced acetylcarnitine accumulation.

Acknowledgments

This research was supported by a Grant-in-Aid for JSPS Fellows (# 24–173, YF) from the Japanese Ministry of Education, Science, Sports

and Culture and a grant-in-aid by the Funding Program for World-Leading Innovative R&D on Science and Technology (#LS102) by the Council for Science and Technology Policy to N.L.F.

The BF-32 antibody developed by Stefano Schiaffino was obtained from the Developmental Studies Hybridoma Bank developed under the auspices of the NICHD and maintained by The University of Iowa, Department of Biology, Iowa City, IA 52242.

Appendix A. Supplementary data

Supplementary data to this article can be found online at http://dx.doi.org/10.1016/j.bbabio.2014.05.356.

References

[1] J. Bremer, Carnitine as a fatty acid carrier in intermediary metabolism, Nature 196 (1962) 993–994.
[2] L.L. Bieber, Carnitine, Annu. Rev. Biochem. 57 (1988) 261–283.
[3] D.M. Muoio, T.R. Koves, Lipid-induced metabolic dysfunction in skeletal muscle, Novartis Found. Symp. 286 (2007) 24–38 (discussion 38–46, 162–3, 196–203).
[4] D.M. Muoio, R.C. Noland, J.-P. Kovalik, S.E. Seiler, M.N. Davies, K.L. DeBalsi, et al., Muscle-specific deletion of carnitine acetyltransferase compromises glucose tolerance and metabolic flexibility, Cell Metab. 15 (2012) 764–777.
[5] R. Wang-Sattler, Z. Yu, C. Herder, A.C. Messias, A. Floegel, Y. He, et al., Novel biomarkers for pre-diabetes identified by metabolomics, Mol. Syst. Biol. 8 (2012) 615.
[6] M.C. Sugden, M.J. Holness, Recent advances in mechanisms regulating glucose oxidation at the level of the pyruvate dehydrogenase complex by PDKs, Am. J. Physiol. Endocrinol. Metab. 284 (2003) E855–E862.
[7] K. Tsintzas, K. Chokkalingam, K. Jewell, L. Norton, I. a Macdonald, D. Constantin-Teodosiu, Elevated free fatty acids attenuate the insulin-induced suppression of PDK4 gene expression in human skeletal muscle: potential role of intramuscular long-chain acyl-coenzyme A, J. Clin. Endocrinol. Metab. 92 (2007) 3967–3972.
[8] M.J. Watt, G.J.F. Heigenhauser, T. Stellingwerff, M. Hargreaves, L.L. Spriet, Carbohydrate ingestion reduces skeletal muscle acetylcarnitine availability but has no effect on substrate phosphorylation at the onset of exercise in man, J. Physiol. 544 (2002) 949–956.
[9] F.B. Stephens, D. Constantin-Teodosiu, P.L. Greenhaff, New insights concerning the role of carnitine in the regulation of fuel metabolism in skeletal muscle, J. Physiol. 581 (2007) 431–444.
[10] P.R. Borum, Carnitine: determination of total carnitine using a radioenzymatic assay, J. Nutr. Biochem. 1 (1990) 111–114.
[11] M. Möder, A. Kießling, H. Löster, Current methods for determination of L-carnitine and acylcarnitines, Monatsh. Chem. Chem. Mon. 136 (2005) 1279–1291.
[12] A.G. Cordente, E. López-Viñas, M.I. Vázquez, J.H. Swiegers, I.S. Pretorius, P. Gómez-Puertas, et al., Redesign of carnitine acetyltransferase specificity by protein engineering, J. Biol. Chem. 279 (2004) 33899–33908.
[13] R.C. Noland, T.R. Koves, S.E. Seiler, H. Lum, R.M. Lust, O. Ilkayeva, et al., Carnitine insufficiency caused by aging and overnutrition compromises mitochondrial performance and metabolic control, J. Biol. Chem. 284 (2009) 22840–22852.
[14] Y. Furuichi, T. Sugiura, Y. Kato, Y. Shimada, K. Masuda, OCTN2 is associated with carnitine transport capacity of rat skeletal muscles, Acta Physiol. (Oxf.) 200 (2010) 57–64.
[15] Y. Furuichi, T. Sugiura, Y. Kato, H. Takakura, Y. Hanai, T. Hashimoto, et al., Muscle contraction increases carnitine uptake via translocation of OCTN2, Biochem. Biophys. Res. Commun. 418 (2012) 774–779.
[16] M.D. Delp, C. Duan, Composition and size of type I, IIA, IID/X, and IIB fibers and citrate synthase activity of rat muscle, J. Appl. Physiol. 80 (1996) 261–270.
[17] M. Takahashi, S. Ueda, H. Misaki, N. Sugiyama, K. Matsumoto, N. Matsuo, et al., Carnitine determination by an enzymatic cycling method with carnitine dehydrogenase, Clin. Chem. 40 (1994) 817–821.
[18] N. Goto-Inoue, Y. Manabe, S. Miyatake, S. Ogino, A. Morishita, T. Hayasaka, et al., Visualization of dynamic change in contraction-induced lipid composition in mouse skeletal muscle by matrix-assisted laser desorption/ionization imaging mass spectrometry, Anal. Bioanal. Chem. 403 (2012) 1863–1871.
[19] P. Challamalla, S. Ghosh, N. Parthiban, K.N.V. Rao, D. Banji, Negative ion mode mass spectrometry—an overview, J. Chem. Biol. Phys. Sci. 2 (2012) 1462–1471.
[20] A. Kubo, M. Ohmura, M. Wakui, T. Harada, S. Kajihara, K. Ogawa, et al., Semi-quantitative analyses of metabolic systems of human colon cancer metastatic xenografts in livers of superimmunodeficient NOG mice, Anal. Bioanal. Chem. 400 (2011) 1895–1904.
[21] T. Hayasaka, N. Goto-Inoue, N. Zaima, Y. Kimura, M. Setou, Organ-specific distributions of lysophosphatidylcholine and triacylglycerol in mouse embryo, Lipids 44 (2009) 837–848.
[22] D.E. Atkinson, The energy charge of the adenylate pool as a regulatory parameter. Interaction with feedback modifiers, Biochemistry 7 (1968) 4030–4034.
[23] D.A. Pirman, R.A. Yost, Quantitative tandem mass spectrometric imaging of endogenous acetyl-L-carnitine from piglet brain tissue using an internal standard, Anal. Chem. 83 (2011) 8575–8581.
[24] S. Schiaffino, L. Gorza, S. Sartore, L. Saggin, S. Ausoni, M. Vianello, et al., Three myosin heavy chain isoforms in type 2 skeletal muscle fibres, J. Muscle Res. Cell Motil. 10 (1989) 197–205.
[25] S. Shimma, Y. Sugiura, T. Hayasaka, Y. Hoshikawa, T. Noda, M. Setou, MALDI-based imaging mass spectrometry revealed abnormal distribution of phospholipids in colon cancer liver metastasis, J. Chromatogr. B Anal. Technol. Biomed. Life Sci. 855 (2007) 98–103.
[26] S. Koizumi, S. Yamamoto, T. Hayasaka, Y. Konishi, M. Yamaguchi-Okada, N. Goto-Inoue, et al., Imaging mass spectrometry revealed the production of lysophosphatidylcholine in the injured ischemic rat brain, Neuroscience 168 (2010) 219–225.
[27] H.-J. Yang, Y. Sugiura, K. Ikegami, Y. Konishi, M. Setou, Axonal gradient of arachidonic acid-containing phosphatidylcholine and its dependence on actin dynamics, J. Biol. Chem. 287 (2012) 5290–5300.
[28] M.D. Vukovich, D.L. Costill, W.J. Fink, Carnitine supplementation: effect on muscle carnitine and glycogen content during exercise, Med. Sci. Sports Exerc. 26 (1994) 1122–1129.
[29] J. Sowell, M. Fuqua, T. Wood, Quantification of Total and Free Carnitine in Human Plasma by Hydrophilic Interaction Liquid Chromatography Tandem Mass Spectrometry, 49 (2011) 463–468.
[30] L. Storlien, N.D. Oakes, D.E. Kelley, Metabolic flexibility, Proc. Nutr. Soc. 63 (2004) 363–368.
[31] D. Constantin-Teodosiu, S. Howell, P.L. Greenhaff, Carnitine metabolism in human muscle fiber types during submaximal dynamic exercise, J. Appl. Physiol. 80 (1996) 1061–1064.
[32] R.B. Armstrong, C.W. Saubert, W.L. Sembrowich, R.E. Shepherd, P.D. Gollnick, Glycogen depletion in rat skeletal muscle fibers at different intensities and durations of exercise, Pflugers Arch. 352 (1974) 243–256.
[33] L.L. Jones, D. a McDonald, P.R. Borum, Acylcarnitines: role in brain. Prog. Lipid Res. 49 (2010) 61–75.